Hydroxide ion Conduction Mechanism in Mg-Al CO_3^{2-} Layered Double Hydroxide

Daiju Kubo[1,2], Kiyoharu Tadanaga[2,3]*, Akitoshi Hayashi[2], and Masahiro Tatsumisago[2]

[1]*Graduate School of Chemical Sciences and Engineering, Hokkaido University, Sapporo, Hokkaido 060-8628, Japan*
[2]*Department of Applied Chemistry, Graduate School of Engineering, Osaka Prefecture University, Sakai, Osaka 599-8531, Japan*
[3]*Faculty of Engineering, Hokkaido University, Sapporo, Hokkaido 060-8628, Japan*

ABSTRACT

Ionic conduction mechanism of Mg-Al layered double hydroxides (LDHs) intercalated with CO_3^{2-} (Mg-Al CO_3^{2-} LDH) was studied. The electromotive force for the water vapor concentration cell using Mg-Al CO_3^{2-} LDH as electrolyte showed water vapor partial pressure dependence and obeyed the Nernst equation, indicating that the hydroxide ion transport number of Mg-Al CO_3^{2-} LDH is almost unity. The ionic conductivity of $Mg(OH)_2$, $MgCO_3$ and $Al_2(CO_3)_3$ was also examined. Only $Al_2(CO_3)_3$ showed high hydroxide ion conductivity of the order of 10^{-4} S cm^{-1} under 80% relative humidity, suggesting that $Al_2(CO_3)_3$ is an ion conducting material and related to the generation of carrier by interaction with water. To discuss the ionic conduction mechanism, Mg-Al CO_3^{2-} LDH having deuterium water as interlayer water (Mg-Al CO_3^{2-} LDH(D_2O)) was prepared. After the adsorbed water molecules on the surface of Mg-Al CO_3^{2-} LDH(D_2O) were removed by drying, DC polarization test for dried Mg-Al CO_3^{2-} LDH(D_2O) was examined. The absorbance attributed to O-D-stretching band for Mg-Al CO_3^{2-} LDH(D_2O) powder at around the positively charged electrode is larger than that before polarization, indicating that the interlayer in Mg-Al CO_3^{2-} LDH is a hydroxide ion conduction channel.

Keywords : Layered Double Hydroxide, Hydroxide Ion Conductor, Ionic Conduction Mechanism, Deuterium Water Replacement

1. Introduction

Two-dimensional(2D) materials are interesting material because of their various unique characteristics. Recently, research on 2D materials such as graphene, 2D-hexagonal BN, and transition metal dichalcogenides, oxides and hydroxides with layered structure is rapidly increasing [1-6]. Among these materials, layered double hydroxides (LDHs) have attracted much attention for various use in a variety of fields, such as catalysts, anion exchange materials and anion conducting materials [7-11]. LDHs are anionic clay and the general formula for LDHs is $[M^{II}_{1-x}M^{III}x(OH)_2][(A^{n-})_{x/n} \cdot mH_2O]$, where M^{II} is a divalent cation, M^{III} is a trivalent cation, and A^{n-} is an anion.

There are several reports on the conductivity of LDH. Kim et al. have reported that Mg-Al LDH showed high ionic conductivity and the conductivity at 200°C under 100% relative humidity reached 3×10^{-2} S cm^{-1} [12]. Mg-Al LDHs intercalated with moderate surfactants show higher conductivity under a dried condition than the conductivity of Mg-Al CO_3^{2-} LDH due to their unique morphology and interaction of water molecules [13,14]. We have been focusing on LDHs as solid-state hydroxide ion conductors for the last decade. We reported that Mg-Al and Ni-Al LDHs intercalated CO_3^{2-} show high hydroxide ion conductivity under high relative humidity (R.H.). We reported that these LDHs can be used as the electrolyte of the alkaline-type direct ethanol fuel cells (DEFCs) and aqueous ammonia fuel cells [15-18]. We also reported the application of LDHs as ionomer for DEFCs and zinc-air secondary battery [19,20]. Ni-Fe LDH played multifunctional roles in the catalyst layer as both a hydroxide ion- and electron- conduc-

tor, and as an electrocatalyst [19,20].

On the other hand, some researchers have reported about solid state anion conductor so far. Ueda et al. have reported that the layered oxides such as $NaCoO_2$ and $KCoO_2$ have hydroxide ion conductivity, and maximum power densities of more than 60 mW cm^{-2} were observed in non-platinum-catalyzed anodes, carbon-only cathodes, and $NaCoO_2$ fuel cells under humidified conditions [21-23]. Hibino et al. have reported that Sb^{5+}-doped SnP$_2$O$_7$ showed high ionic conductivity on the order of 10^{-2} S cm^{-1} under humidification [24-26]. Sadakiyo et al. have reported that alkylammonium hydroxides introduced alkaline stable zeolitic imidazolate framework showed hydroxide ion conduction [27]. Thus, in addition to LDH, various other hydroxide ion conducting solid materials have been found. However, there are few studies about hydroxide ion conducting mechanism in hydroxide ion conducting materials. Recently, Sun *et al.* have reported that the hydroxide ion conduction in LDHs is anisotropic, and in-plane hydroxide ion conductivity is much higher than cross-plane conductivity [28]. However, hydroxide ion conduction in LDHs has not been well-known yet and should be clarified for the improvement the ionic conductivity and cell performance.

In this study, Mg-Al CO_3^{2-} LDH (H_2O) and Mg-Al CO_3^{2-} LDH (D_2O), in which deuterium water was introduced as interlayer water molecules, were prepared. The transport number and ion conducting species of LDHs were examined. To investigate the carrier generation source in LDHs, the electrochemical properties for Mg-Al LDHs-related compounds, $Mg(OH)_2$, $MgCO_3$ and $Al_2(CO_3)_3$, were examined. In addition, the DC polarization behavior of Mg-Al CO_3^{2-} LDH(D_2O) was examined to discuss the ion conducting path.

2. Experimental

Mg-Al CO_3^{2-} LDH was prepared by using the co-precipitation process, as described in previous papers [15,16]. Mg-Al CO_3^{2-} LDH (D_2O) was prepared through the reconstructing process [29]. Mg-Al CO_3^{2-} LDH obtained by the co-precipitation process was calcined at 500ºC for 5 h to form a mixed magnesium-aluminum oxide. Then, the mixed oxide powders were dispersed in 4M Na_2CO_3-D_2O under N_2 flow. The mixed oxide was rehydrated in 4M Na$_2$.

CO_3- D_2O. The solution was stirred at R.T. for 24 h under N_2 flow condition. After stirring, the obtained powders were filtered under a N_2 flow and dried in vacuum.

In this study, to investigate carrier-generation source and ion conduction path in LDHs, the ionic conductivity of $Mg(OH)_2$, $MgCO_3$ and $Al_2(CO_3)_3$, which are the structurally- and compositionally-related compounds of Mg-Al CO_3^{2-} LDH, was evaluated for comparison. The aim of this experiment is to clarify primarily responsible structural features in the carrier generation and conduction path of the ionic conduction. Conducting ion species and transport number were examined using a water vapor concentration cell using Mg-Al CO_3^{2-} LDHs as the separator [15]. The pelletized Mg-Al CO_3^{2-} LDH with the thickness of about 300 μm was sandwiched with a pair of Pt-loaded carbon sheets. The Pt loading amount of carbon sheet is 1.9 mg/cm^2. The electromotive force (EMF) of the cell was measured by exposing a flow of humidified N_2/O_2 gas with different water vapor pressures to one side of the separator and N_2/O_2 gas with 10% R.H. to the other side.

The ionic conductivities of Mg-Al LDHs were determined using impedance spectra in a frequency range of 1 Hz to 8×10^6 Hz under H_2O or D_2O atmosphere [15,18] (Solartron 1260; Solartron Analytical). The conductivity was measured more than 30 min after the chamber reached a humidified atmosphere to obtain stabilized conductivity.

X-ray diffraction (XRD) patterns were measured to identify crystalline phases (XRD 6000; SHIMAZU Corp.). The amount of CO_3^{2-} and replacement of H_2O with D_2O were confirmed using Thermogravimetry Mass spectroscopy (TG-MS) (M-400QA-M;CANON ANELVA Corp.).

DC polarization test was carried out using the blocking electrode at 0.5V for 3 h in a dry box. Mg-Al CO_3^{2-} LDH(D_2O) was dried at 100ºC for 1 h in advance. DC was applied to the pelletized Mg-Al CO_3^{2-} LDH (D_2O), and powders of DC polarized Mg-Al CO_3^{2-} LDH (D_2O) pellet at around the electrodes were examined using Fourier transform infrared (FT-IR) spectra (Spectrum GX; PERKINELMER).

3. Results and Discussion

Fig. 1 shows XRD patterns of Mg-Al CO_3^{2-} LDH (H_2O), mixed magnesium-aluminum oxide obtained
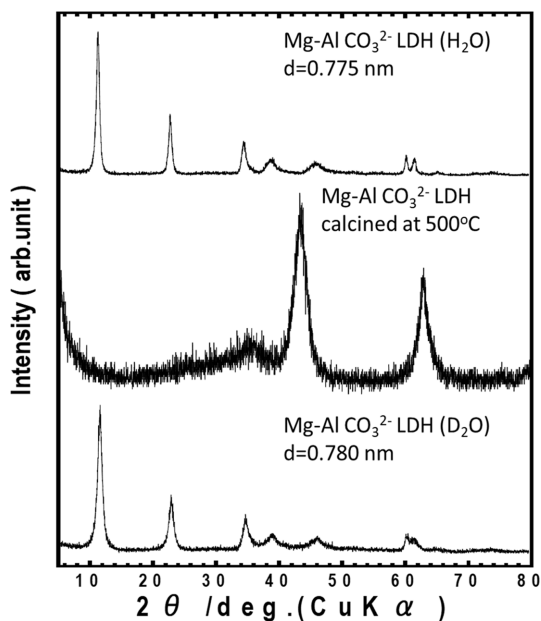
Fig. 1. XRD patterns of Mg-Al CO_3^{2-} LDH(H_2O), Mg-Al CO_3^{2-} LDH (H_2O) calcined at 500°C and Mg-Al CO_3^{2-} LDH(D_2O) obtained by reconstructing calcined Mg-Al CO_3^{2-} LDH in 4M Na_2CO_3-D_2O.

Fig. 2. MS spectra of Mg-Al CO_3^{2-} LDH(D_2O). Square (□) :H_2O, Circle (●): D_2O, Triangle (△): CO_2

by calcining Mg-Al CO_3^{2-} LDH (H_2O) at 500°C, and restructured Mg-Al CO_3^{2-} LDH (D_2O). After the sample is calcined at 500°C, the characteristic 003, 006 reflections based on the layered structure disappeared, indicating that the layered structure is collapsed by calcination. The XRD patterns of Mg-Al CO_3^{2-} LDH (H_2O) and Mg-Al CO_3^{2-} LDH (D_2O) showed characteristic 003, 006 reflections. The basal spacing of Mg-Al CO_3^{2-} LDH (D_2O) is slightly larger than that of Mg-Al CO_3^{2-} LDH (H_2O), indicating that interlayer water was replaced with deuterium oxide, which is larger than water molecule.

Fig. 2 shows TG-MS spectra of Mg-Al CO_3^{2-} LDH (D_2O) after drying at 100 °C. Previously, we reported on the thermal degradation behavior of Mg-Al CO_3^{2-} LDH [30]. The weight loss at temperatures below 100°C is assigned to the loss of the adsorbed water on LDH. The weight loss at temperatures from 100°C to 250°C is assigned to the loss of interlayer water in LDH, and the weight loss at higher temperature is assigned to the elimination of H_2O from OH groups in the inorganic layer and CO_2 form CO_3^{2-}. The TG-MS spectra for Mg-Al CO_3^{2-} LDH (D_2O) showed a good correlation with previous DTA-TG results.
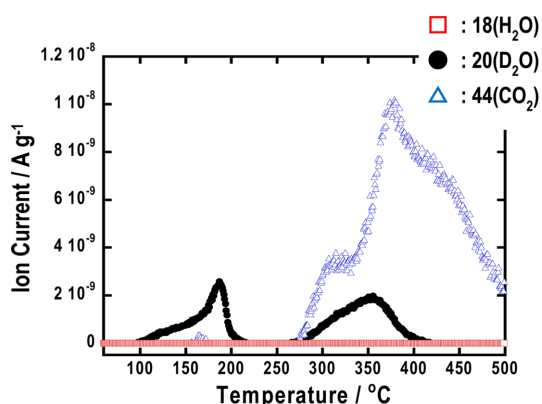
Weight loss attributed to D_2O (m/z=20) was observed from 100°C to 250°C and at temperatures above 250°C. Weight loss attributed to CO_2(m/z=44) was observed at temperatures above 250°C. On the other hand, weight loss attributed to H_2O (m/z=18) was not observed, indicating that interlayer water molecule in Mg-Al CO_3^{2-} LDH (H_2O) was replaced with D_2O and hydroxy groups in LDH were OD groups. Thus, formation of Mg-Al CO_3^{2-} LDH (D_2O) was confirmed.

Temperature dependence of ionic conductivity for Mg-Al CO_3^{2-} LDH under 80%R.H. with H_2O and D_2O is shown in Fig. 3. In the measurement under D_2O, the chamber was humidified with D_2O. The ionic conductivity of Mg-Al CO_3^{2-} LDH under H_2O condition showed 2.7×10^{-3} S cm^{-1} at 80°C. On the other hand, the ionic conductivity of Mg-Al CO_3^{2-} LDH under D_2O condition showed 2.4×10^{-3} S cm^{-1} at 80°C. The ionic conductivity ratio is 1:0.91 (in H_2O : in D_2O). In previous reports, we reported that the ionic conductivity of LDHs depends on its their hydration state. The hydroxide ion conduction in LDHs needs humidified conditions and is supposed to be based on the Grotthuss mechanism through the water in the atmosphere. If LDHs are a proton conducting material, the ionic conductivity ratio is the same of the molecular amount: the ratio should be 1 : 0.5 (H^+ : D^+). On the other hand, if LDHs are hydroxide ion conducting material, the ionic conductivity ratio should be 1: 0.94 (OH^-: OD^-), which is in good agreement with the observed conductivity ratio. Thus, this result strongly suggests that Mg-Al CO_3^{2-} LDH is hydroxide ion conductor. Moreover, it should
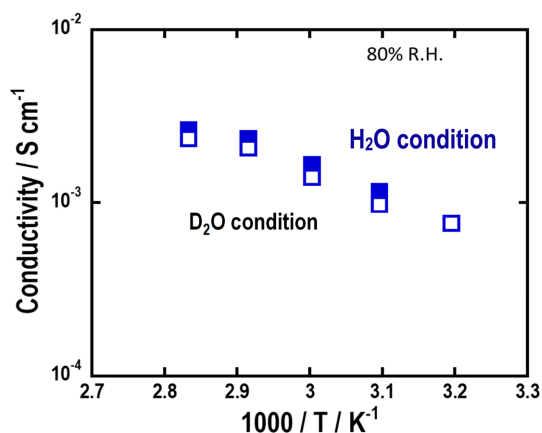
Fig. 3. Temperature dependence of ionic conductivity of Mg-Al CO_3^{2-} LDH under H_2O(■) and D_2O(□) humidified condition.

Fig. 4. Partial pressure dependence of water vapor concentration cell using Mg-Al CO_3^{2-} LDH as electrolyte. pH_2O^I: water vapor partial pressure at dry side pH_2O^{II}: water vapor partial pressure at wet side

be discussed about the contribution on each conduction path. In our previous report, the relative humidity (R.H.) dependence of ionic conductivity was reported [12], and the conductivities increase with an increase in RH and temperature. The amount of adsorbed water at the surface of LDH must increase with increased RH. Thus, the surface conduction in LDH will proceed smoothly and the grain boundary resistance will decrease. Moreover, it is clear that the activation energy under low humidified condition and high humidified condition is different, indicating that the dominant conducting path is different and the interlayer path seems to become dominant under low humidified conditions.

To investigate the hydroxide ion transport number, the water vapor concentration cell using Mg-Al CO_3^{2-} LDH (H_2O) as electrolyte was fabricated. As stated in our previous reports, the water vapor concentration cell results proved that Mg-Al CO_3^{2-} LDHs are hydroxide ion conductor [12], and the all solid-state alkaline fuel cell using Mg-Al CO_3^{2-} LDH as electrolyte was operated [12,14,15]. However, the hydroxide ion transport number of LDHs has not been discussed so far. Thus, the transport number of LDHs was determined by the water vapor concentration cell with different water-vapor pressure.

The reactions for the anion (OH^-) conductor at the electrodes of water vapor concentration cell are described as follows [12].
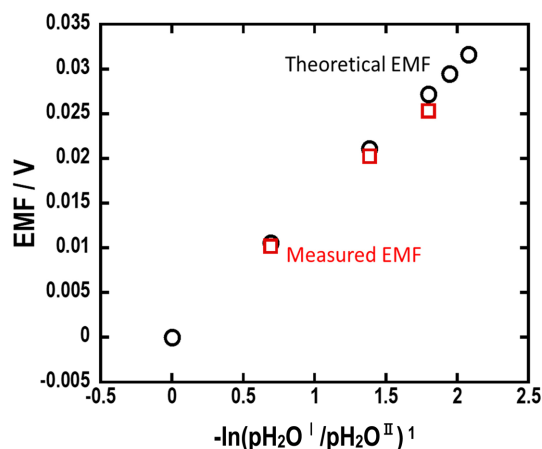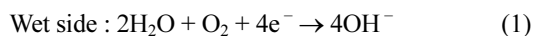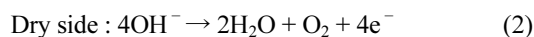
$$\text{Wet side} : 2H_2O + O_2 + 4e^- \rightarrow 4OH^- \tag{1}$$

$$\text{Dry side} : 4OH^- \rightarrow 2H_2O + O_2 + 4e^- \tag{2}$$

In case that above reaction proceeds, the following Nernst equation is considered.

$$E = RT/2F \cdot \ln(pH_2O^I/pH_2O^{II}) \tag{3}$$

The relative humidity in the dry side is controlled at 10 %R.H., and then, the EMF of the cell at each water vapor partial pressure was measured by changing the relative humidity in the wet side.

Partial pressure dependence of the measured and theoretical EMF of the water vapor concentration cell using Mg-Al CO_3^{2-} LDH as electrolyte is shown in Fig. 4. The measured EMF of the cell showed the same trend as the theoretical EMF of the Nernst equation. The transport number is calculated by the proportion of the measured EMF to the theoretical EMF. The hydroxide ion transport number of Mg-Al CO_3^{2-} LDH is estimated to be from 0.91 to 0.95, indicating that the dominant conducting ion species of Mg-Al CO_3^{2-} LDH are hydroxide ion.

To investigate the source of hydroxide ions in LDHs, the ionic conductivity of the Mg-Al LDH-related compounds ($Mg(OH)_2$ (brucite, layered structure), $MgCO_3$ (spherical powder), $Al_2(CO_3)_3$ (spherical powder), and the mixture of $Mg(OH)_2$ and $Al_2(CO_3)_3$ with Mg/Al=3) was measured. Temperature dependence of ionic conductivity of these com-
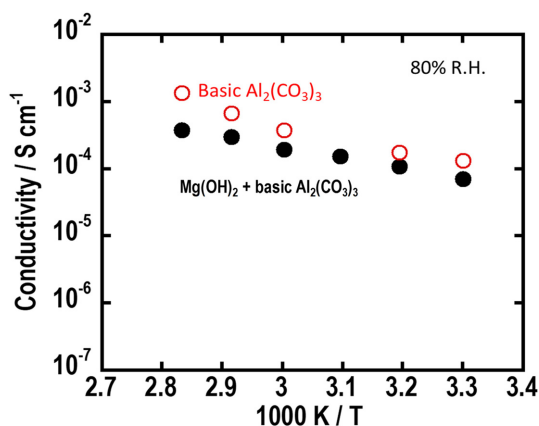
Fig. 5. Temperature dependence of the ionic conductivity of $Al_2(CO_3)_3$ and the mixture of $Mg(OH)_2$ and $Al_2(CO_3)_3$ under 80%R.H.

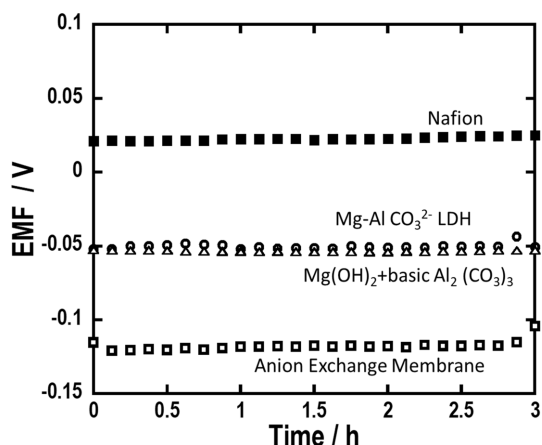**Fig. 6.** Variation of electromotive force(EMF) under 80%R.H..(■:Nafion, ○:Mg-Al CO_3^{2-} LDH, △:Mg(OH)$_2$ +basic $Al_2(CO_3)_3$, □:Anion Exchange Membrane)

pounds is shown in Fig. 5. The conductivity of $Mg(OH)_2$ and $MgCO_3$ was below the measurement limit (less than 10^{-10} S cm^{-1}) under 80%R.H., suggesting that simple metal hydroxides with layered structure or carbonate salts with the basic element do not have conducing ion species. On the other hand, $Al_2(CO_3)_3$ and the mixture of $Mg(OH)_2$ and $Al_2(CO_3)_3$ showed rather high ionic conductivity of the order of 10^{-4} S cm^{-1} under 80%R.H., indicating that $Al_2(CO_3)_3$ is an ion conducting material and related to the generation of carrier.

The water vapor concentration cell using these compounds as electrolyte was fabricated and measured EMF of these cells. Fig. 6 shows the EMF for the water vapor concentration cell using these compounds as electrolyte. The EMF of the cell using the cation exchange membrane is positive, whereas that of the cell using the mixture of $Mg(OH)_2$ and $Al_2(CO_3)_3$ and the anion exchange membrane as well as Mg-Al CO_3^{2-} LDH is negative, indicating that $Al_2(CO_3)_3$ is an anion conducting material and the interaction between $Al_2(CO_3)_3$ and water in the atmosphere generates hydroxide ion as below reaction.

$$CO_3^{2-} + H_2O \rightarrow HCO_3^- + OH^- \tag{4}$$
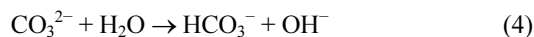
Mg-Al CO_3^{2-} LDH consists of cationic hydroxide layers and carbonate anion located in the interlayer space for charge compensation of the positively charged hydroxide layers. The located carbonate anion could generate hydroxide ion carrier in Mg-Al CO_3^{2-} LDH.

On the other hand, Mg-Al CO_3^{2-} LDH shows higher hydroxide ion conductivity of the order of the 10^{-3} S cm^{-1} under 80%R.H. than that of the mixture of $Mg(OH)_2$ and $Al_2(CO_3)_3$. In this experiment, the specific surface area and molar ratio of Mg/Al (Mg/ Al=3), which are related to the amount of carrier, were almost the same. Therefore, the structural difference between Mg-Al CO_3^{2-} LDH and the mixture of $Mg(OH)_2$ and $Al_2(CO_3)_3$ should be attributed to the difference in hydroxide ion conduction: $Mg(OH)_2$ has layered structure like LDH but has no carrier. $Al_2(CO_3)_3$ has no layered structure but has ion conducting carrier. Mg-Al CO_3^{2-} LDH has both layered structure and ion conducting carrier.

To examine the conduction path in Mg-Al LDHs, DC polarization test was performed. To reduce the effects of adsorbed water molecule on the surface, Mg-Al CO_3^{2-} LDH(D$_2$O) was dried at 100°C for 1 h in advance. DC (0.5V) was applied to the pelletized Mg-Al CO_3^{2-} LDH (D$_2$O), and IR spectra were measured for the polarized Mg-Al CO_3^{2-} LDH(D$_2$O) powders. The IR spectra of the power at around the positive electrode and the negative electrode are shown in Fig. 7. The band in the range from 2500 cm^{-1} to 2700 cm^{-1} is attributed to O-D-stretching [31]. The band in the range from 550 cm^{-1} to 800 cm^{-1} is attributed to Mg-O and Al-O-stretching. The absorbance of O-D-stretching bands and Mg-O

Table 1. Absorbance for O-D stretching band and Mg-O, Al-O stretching band of Mg-Al CO_3^{2-} LDH(D_2O), before and after DC polarization

	Absorbance (O-D)	Absorbance (Mg-O, Al-O)	Abs(O-D)/Abs(Mg-O, Al-O)
Mg-Al LDH reconstructed in D_2O (before DC polarization)	0.027	0.478	0.057
Positive electrode side (after DC polarization)	0.030	0.482	0.062
Negative electrode side (after DC polarization)	0.026	0.484	0.052
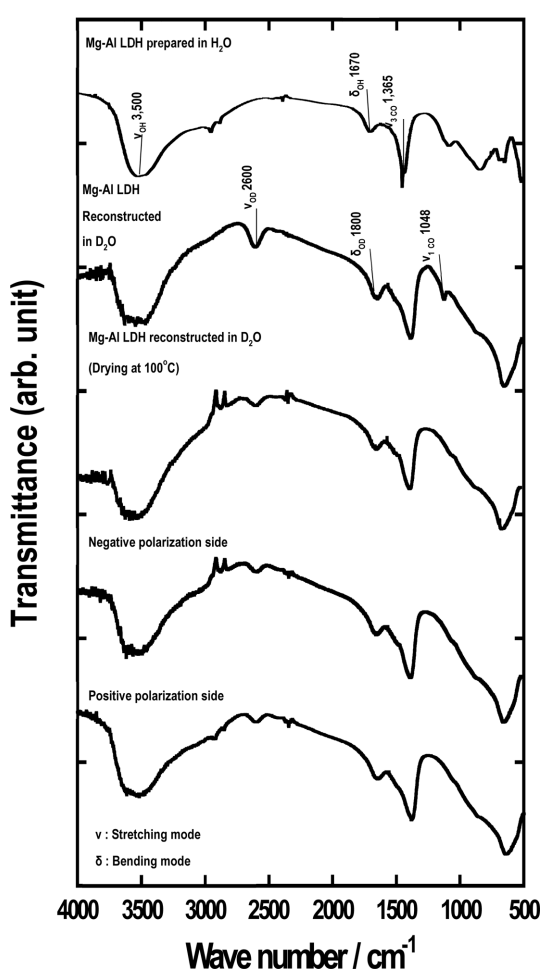
Fig. 7. IR spectra of Mg-Al CO_3^{2-} LDH(H_2O), Mg-Al CO_3^{2-} LDH(D_2O), and Mg-Al CO_3^{2-} LDH(D_2O) before and after DC polarization.

and Al-O-stretching bands are shown in Table 1. The absorbance attributed to O-D-stretching band for Mg-Al CO_3^{2-} LDH(D_2O) at the positive electrode surface is larger than that before polarization. The absorbance attributed to O-D-stretching band for Mg-Al CO_3^{2-} LDH(D_2O) at the negative electrode surface is smaller than that before polarization. These results show that OD⁻ ions are moved by the DC polarization. Because the adsorbed water molecules on the surface was removed in advance, the surface conduction can be ignored in this experiment, and the interlayer with D_2O and CO_3^{2-} should be the only ion conduction path. Thus, the DC polarization result indicates that deuterium hydroxide ions move through the interlayer of Mg-Al CO_3^{2-} LDH(D_2O), probably by the Grotthus mechanism with D_2O in the interlayer. The high hydroxide ion conduction in LDH must be because of not only the attribution of the surface conduction but also the interlayer conduction.

4. Conclusions

The partial pressure dependence for the water vapor concentration cell shows that the anion transport number of Mg-Al CO_3^{2-} LDH is between 0.91 and 0.95, indicating that the dominant ion conducting species is hydroxide ions. $Mg(OH)_2$ and $Mg(CO_3)$ did not show ion conduction but $Al_2(CO_3)_3$ showed hydroxide ion conduction under 80% relative humidity. The hydroxide ion source is supposed to be the interaction of $Al_2(CO_3)_3$ and water molecules. Mg-Al CO_3^{2-} LDH(D_2O) was prepared by the reconstructing process and confirmed that interlayer water was replaced with D_2O. The ionic conduction measurement under D_2O humidity and DC polarization test in Mg-Al CO_3^{2-} LDH(D_2O) prove that the interlayer D_2O has large contribution to the ionic conduction, indicating that the LDH hydroxide ion conducting path is not only surface conduction but also interlayer conduction and consequently, and the high hydroxide

ion conductivity for LDHs must be observed. LDHs with surface and interlayer conduction path are expected for the application in electrolyte and ionomer for alkaline fuel cells because of the high hydroxide ion conduction and durability.

Acknowledgments

References

[1] X. Huang, Z. Zeng and H. Zhang, *Chem. Soc. Rev.*, **2013**, *42(5)*, 1934.

[2] D. Chen, L. Tang and J. Li, *Chem. Soc. Rev.*, **2010**, *39(8)*, 3157-3180.

[3] K. F. Mak and J. Shan, *Nat. Photonics*, **2016**, *10(4)*, 216-226.

[4] K. S. Novoselov, A.K. Geim, S.V. Morozov, D. Jiang, Y. Zhang, S.V. Dubonos, I.V. Grigorieva, A. A. Firsov, *Science*, **2004**, *306(5696)*, 666-669.

[5] W. Choi, N. Choudhary, G. H. Han, J. Park, D. Akinwande and H. Lee, *Materials Today*, **2017**, *20(3)*, 116-130.

[6] Y. Lin and J. W. Connell, *Nanoscale*, **2012**, *4(22)*, 6908.

[7] J. Zhang, J. Liu, L. Xi, Y. Yu, N. Chen, S. Sun, W. Wang, K. M. Lange and B. Zhang, *J. Am. Chem. Soc.*, **2018**, *140(11)*, 3876-3879.

[8] L. Zeng, T. S. Zhao, *Nano Energy*, **2015**, *11*, 110-118.

[9] Q. Wang, D. O'Hare, *Chem. Rev.*, **2012**, *112(7)*, 4124-4155.

[10] Z. Liu, R. Ma, M. Osada, N. Iyi, Y. Ebina, K. Takada, T. Sasaki, *J. Am. Chem. Soc.*, **2006**, *128(14)*, 4872-4880.

[11] Y. Li, M. Gong, Y. Liang, J. Feng, J. Kim, H. Wang, G. Hong, B. Zhang, H. Dai, *Nat. Commun.*, **2013**, *4(1)*, 1805.

[12] H. S. Kim, Y. Yamazaki, J. D. Kim, T. Kudo, and I. Honma, *Solid State Ionics*, **2010**, *181(19-20)*, 883.

[13] P. Zhang, S. Sago, T. Yamaguchi, G. M. Anilkumar, *J. Power Sources,* **2013**, *230*, 225-229.

[14] J. P. Maria, R. de M. Bruno, N. Spyridon, C.F. Fabio, C.T. Ana, *J. Nanopart Res.*, **2013**, *15(2)*, 1-14.

[15] K. Tadanaga, Y. Furukawa, A. Hayashi, M. Tatsumisago, *Adv. Mater.*, **2010**, *22(39)*, 4401–4403.

[16] Y. Furukawa, K. Tadanaga, A. Hayashi and M. Tatsumisago, *Solid State Ionics*, **2011**, *192(1)*, 185-187.

[17] D. Kubo, K. Tadanaga, A. Hayashi, M. Tatsumisago, *J. Electroanal. Chem.* **2012**, *671*, 102-105.

[18] S. Ishiyama, N.C. Rosero-Navarro, A. Miura, K. Tadanaga, *Mater. Res. Bull.*, **2019**, *119*, 110561.

[19] D. Kubo, K. Tadanaga, A. Hayashi, M. Tatsumisago, J. Power Sources, **2013**, *222*, 493-497.

[20] D. Kubo, K. Tadanaga, A. Hayashi, M. Tatsumisago, *J. Mater. Chem. A*, **2013**, *1(23)*, 6804-6809.

[21] T. Takeguchi, H. Takahashi, T. Yamanaka, A. Nakamura, W. Ueda, *ECS Trans.*, **2010**, *33(1),* 1847-1851.

[22] H. Takahashi, T. Takeguchi, T. Yamanaka, T. Kyomen, M. Hanaya, W. Ueda, *ECS Trans.*, **2010**, *33(1)*, 1861-1866.

[23] M. Matsuda, T. Murota, H. Takahashi, T. Takeguchi, W. Ueda, *ECS Trans.*, **2010**, *33(1)*, 1831-1836.

[24] T. Hibino, Y. Shen, M. Nishida, and M. Nagao, *Angew. Chem. Int. Ed.*, **2012**, *124(42),* 10944-10948.

[25] T. Hibino, K. Kobayashi, *J. Mater. Chem. A,* **2013**, *1(4)*, 1134.

[26] T. Hibino, K. Kobayashi, *J. Mater. Chem. A,* **2013**, *1(23)*, 6934.

[27] M. Sadakiyo, H. Kasai, K. Kato, M. Takata, M. Yamauchi, *J. Am. Chem.Soc.*, **2014**, *136(5)*, 1702-1705.

[28] P. Sun, R. Ma, X. Bai, K. Wang, H. Zhu, T. Sasaki, *Sci. Adv.*, **2017**, *3(4)*, e1602629.

[29] J. Rocha, M. del Arco, V. Rives, M. A. Ulibarri, *J. Mater. Chem.,* **1999**, *9(10)*, 2499-2503.

[30] K. Tadanaga, Y. Furukawa, A. Hayashi, M. Tatsumisago, *J. Electrochem. Soc.*, **2012**, *159(4)*, B368.

[31] J.T. Kloprogge, L. Hickey, R. L. Frost, *J. Mater. Sci.*, **2002**, *21*, 603-605.